Electronic Supporting Information

Experimental section

Synthetic procedures

Materials. All chemical reagents were purchased and used without further purification: potassium ferricyanide (Acros Organics, 99%), Gold(I) potassium cyanide (Alfa Aesar), Nickel(II) chloride hexahydrate (Chimica, 99%), Potassium borohydride (Acros Organics, 98%), Thalium nitrate ($TlNO_3$, 88.99%, Sigma-Aldrich)), Iron(III) chloride hexahydrate ($FeCl_3{\cdot}6H_2O$, 97% Chimica), (4-(2-hydroxyethyl)-1-piperazineethanesulfonic acid) (Hepes, Sigma-Aldrich), Dextran (M_w = 6000 g/mol, Sigma-Aldrich) 1,2-dimyristoyl-sn-glycero-3-phosphocholine (DMPC, Avanti polar lipids), ultra-pure water. The $Na_3[Fe(CN)_6]$ complex was obtained by passing the $K_3[Fe(CN)_6]$ through an ion-exchange resin (acidic form) followed by neutralisation with NaOH.

Synthesis of PB nanoparticles 1. At 25 °C, aqueous solutions of $FeCl_3{\cdot}6H_2O$ (10 mM, 10 mL) and $Na_4[Fe(CN)_6]10H_2O$ (11.25 mM, 10 mL) were added simultaneously to 100 mL of pure water at 2 mL/h rate, using a syringe pump. After completion of the addition, the mixture was stirred one hour before being centrifuged at 35,700 x g (20,000 rpm) during 10 min. The supernatant was removed and the NPs were washed successively with water and ethanol and dried under vacuum.
IR (KBr): ν(O-H) = 3630 cm^{-1} (coordinate water), ν(O-H) = 3420 cm^{-1} (crystalized water), ν(C≡N) = 2080 cm^{-1} (Fe^{III}–C≡N–Fe^{II}), δ(O–H) = 1605 cm^{-1} (crystallized water), ν(Fe^{II}-CN) = 600 cm^{-1}, δ(Fe^{II}-CN) = 496 cm^{-1}. EDS: 10.65/89.35 (Na/Fe). Formula found: $Na_{0.10}Fe[Fe(CN)_6]_{0.77}$.

Synthesis of double layered Au@PB core@shell nanoheterostructures 2. In a typical experiment for the synthesis of pristine gold nanoparticles of around 20 nm, KBH_4 (0.63 mmol) was added to 100 mL of an aqueous solution of $K[Au(CN)_2]$ ($4.8.10^{-5}$ mol, $4.8.10^{-4}$ M) under vigorous stirring at 25 °C. The colorless solution rapidly turned red, indicating the formation of NPs. After 20 min, 2 mL of an aqueous solution of $Na_3[Fe(CN)_6]$ (5.65 mM) and 2 mL of an aqueous solution of $NiCl_2{\cdot}6H_2O$ (5.00 mM) were simultaneously added (2 mL/h) to the gold NPs solution under vigorous stirring at 25 °C. After completion of the addition, the solution was vigorously stirred for one hour. Then the pH of the solution of NPs was decreased close to 4 with addition of HCl (1 M). The aqueous solution of NPs was centrifuged at 35,700 × g (20,000 rpm) during 5 min. The supernatant was removed and the NPs were dispersed in 100 mL of water. Then, 8 mL of an aqueous solution of $Na_4[Fe(CN)_6]{\cdot}10H_2O$ (5.65 mM) and 8 mL of an aqueous solution of $FeCl_3{\cdot}6H_2O$ (5.0 mM) were simultaneously added (2 mL/h) under vigorous stirring at 25 °C. After the addition, the solution was vigorously stirred for one hour. The aqueous solution of NPs was centrifuged at 35,700 × g (20,000 rpm) during 10 min. The supernatant was removed and the NPs were washed successively with water and ethanol and dried under vacuum.
Dark Blue powder. IR (KBr): ν(O-H) = 3620 cm^{-1} (coordinate water), ν(O-H) = 3410 cm^{-1} (crystalized water), ν(C≡N) = 2080 cm^{-1} (Fe^{III}–C≡N–Fe^{II}), δ(O–H) = 1609 cm^{-1} (crystallized water), ν(Fe^{II}-CN) = 600 cm^{-1}, δ(Fe^{II}-CN) = 499 cm^{-1}. EDS: 1. 1/1.0/59.8/3.9/34.2 (Na/K/Fe/Ni/Au). Formula found: $Au_{8.70}@Na_{0.27}Ni[Fe(CN)_6]_{0.63}@Fe_{8.30}[Fe(CN)_6]_{6.20}$.

Post-synthetic grafting of PB and Au@PB core@shell nanoheterostructures with dextran (sample 1a and 2a, respectively). For both samples, the grafting was performed by mixing the pristine NPs with the dextran (6000 $g.mol^{-1}$) with a stoichiometry 1:1 in water for 24 h under stirring.

Then, the solution was centrifuged at 35,700 × g (20,000 rpm) during 10 min. The supernatant was removed and the NPs were washed with water and dried under vacuum.
IR (KBr): ν(O-H) = 3630 cm^{-1} (coordinate water), ν(O-H) = 3420 cm^{-1} (crystalized water/primary alcohol groups), ν(C-H) = 2920-2875 cm^{-1} (aliphatic), ν(C≡N) = 2080 cm^{-1} (Fe^{III}–C≡N−Fe^{II}), δ(O–H) = 1605 cm^{-1} (crystallized water), δ(O–H) = 1455–1355 cm^{-1}, ν(C-O) = 1156 cm^{-1} (primary alcohol groups), ν(C-O) = 1020 cm^{-1} (ether oxide), ν(Fe^{II}-CN) = 600 cm^{-1}, δ(Fe^{II}-CN) = 496 cm^{-1}.

Post-synthetic coating of PB and Au@PB nanoparticles with lipid bilayers (1b and 2b, respectively). Small unilamellar vesicles (SUVs) were prepared following Bangham's method. Briefly, a dry lipid film was prepared from a lipid stock solution (stored at 5 $mg.mL^{-1}$ in chloroform at –20 °C). The dry lipid film at the bottom of a roundish glass tube was obtained by solvent evaporation under nitrogen flow and was kept under vacuum overnight. The lipid film was hydrated in Hepes-buffered saline (HBS, NaCl 150 mM, Hepes 20 mM) at 2 $mg.mL^{-1}$ of lipids and vortexed for 5 min. SUVs were obtained by extrusion through polycarbonates membranes. Lipid suspension was passed back and forth approximately 15 times through 100 nm pores and 25 times through 50 nm pores. The resulting SUVs have a hydrodynamic diameter of 83.5 ± 4.4 nm with a polydispersity index of 0.1 ± 0.04 and a zeta potential of –3.7 ± 2.4 mV. For lipid coating, NPs were dispersed ultrasonically (35 W, 35 kHz) for 2 minutes at 5 $mg.mL^{-1}$ in water (Millipore, 18 MΩ.cm). 100 µL NPs dispersion was added to 0.4 mL of 2 $mg.mL^{-1}$ SUV suspension (corresponding to a surface area ratio 8/1 SUVs/NPs). This mixture was vortexed for 1 min and sonicated in ultrasound bath for 1 min. Rotating agitation of the sample was performed for 3 hours at 37 °C. Lipid coated DMPC NPs were then isolated by 4 centrifugation steps (4,000 × g, 20 minutes), to remove exceeding SUVs.
IR (KBr): ν(O-H) = 3620 cm^{-1} (coordinate water), ν(O-H) = 3410 cm^{-1} (crystalized water), ν(C-H) = 2960-2850 cm^{-1} (aliphatic), ν(C≡N) = 2080 cm^{-1} (Fe^{III}–C≡N−Fe^{II}), ν(C=O) = 1740 cm^{-1} (ester), ν(C=C) = 1650 cm^{-1} (alcene), δ(O–H) = 1609 cm^{-1} (crystalized water), ν(=C-H) = 1460 cm^{-1}, ν(PO^{2-}) = 1255 cm^{-1} , ν(C-N) = 1165 cm^{-1} , ν(C-O) = 1090 cm^{-1} , ν(P-O-C) = 980, 790 cm^{-1} , ν(Fe^{II}-CN) = 601 cm^{-1}, δ(Fe^{II}-CN) = 499 cm^{-1}.

Thallium capture experiments. Tl^+ sorption experiments on NPs were performed by using non-radioactive Tl^+ containing solutions in order to investigate the sorption kinetic. All Tl^+ insertion experiments (kinetic sorption and isotherm sorption studies) were performed in batch solution under stirring at room temperature. For the kinetic sorption studies, the NPs were dispersed by sonication in a determined concentration of an aqueous solution of $TlNO_3$. The solution was stirred for different period of time from 1 h to 24 h, then centrifuged at 35,700 × g (20,000 rpm) during 10 min. The supernatant was removed and the NPs were washed several times to eliminate non adsorbed Tl^+, successively with water and ethanol, and dried under vacuum. The sorption isotherm's measurements were plotted from data obtained at reaction equilibrium (24 h) with different concentrations of TlCl solution.
Nanoparticles Tl^+/PB/dextran. The Tl^+ containing NPs were obtained by simple mixing of PB NPs with an aqueous solution of $TlNO_3$ (6.0 10^{-4} M for the kinetic studies, from 3.0 10^{-4} M to 8.4×10^{-3} M for the isotherm studies). The final Tl^+ containing NPs were centrifuged and washed several times with water and ethanol. Estimated formula for the maximum of inserted Tl: $Tl_{0.22}Na_{0.03}Fe[Fe(CN)_6]_{0.81}$.
Core@shell nanoparticles Au@Tl^+/PB/dextran. The Tl^+ containing NPs were obtained by simple mixing of core@shell NPs with an aqueous solution of $TlNO_3$ (4.0 10^{-4} M for the kinetic studies, from 4.0 10^{-4} M to 5.0 10^{-3} M for the isotherm studies). The final Tl^+ containing NPs were centrifuged and washed several times with water and ethanol. Estimated formula for the maximum of inserted Tl: $Au_{8.7}@Na_{0.27}Ni[Fe(CN)_6]_{0.63}@Tl_{1.8}Fe_{8.3}[Fe(CN)_6]_{6.2}$.

Preparation of nanoprobes for SPECT/CT experiments.

Preparation of PB/dextran (1a) and Au@PB/dextran (2a) nanoparticles for SPECT/CT measurements (samples $^{201}Tl^{+}$/1a and **$^{201}Tl^{+}$/2a**, respectively**).** ^{201}TlCl was obtained from CisBio, and nanoparticles were radio-labelled at the activity of 10 MBq per mg of NP. In a typical experiment, 2 mg of the studied nanoparticles, either $NaFe^{III}[Fe^{II}(CN)_6]$/dextran **1a**, and $Au@NaNi[Fe^{II}(CN)_6]@NaFe^{III}[Fe^{II}(CN)_6]$/dextran **1b** were treated with 2 mL of 10 MBq.mL^{-1} ^{201}TlCl aqueous solution in order to obtain **$^{201}Tl^{+}$/1a** and **$^{201}Tl^{+}$/2a** nanoprobes.

Preparation of PB/lipid bilayers 1b nanoparticles for SPECT/CT experiments ($^{201}Tl^{+}$/1b). The $NaFe^{III}[Fe^{II}(CN)_6]$/lipids bilayers **1b** requiring to stay in aqueous media for the lipid bilayer integrity, 250 µL of a solution containing 2 mg of the studied nanoparticles in of 0.9 % NaCl was treated with 750 µL of a 10 MBq mL^{-1} ^{201}TlCl aqueous solution in order to obtain **$^{201}Tl^{+}$/1b**.

SPECT-CT imaging. All animal experiments were performed in compliance with the guidelines of the French government and the standards of Institut National de la Santé et de la Recherche Médicale for experimental animal studies (agreement C34-172-27).

Mice (Nude athymic FoxN1) were obtained from Harlan Laboratories and were acclimated for one week before experimental use. They were housed at 22 °C and 55% humidity with a light–dark cycle of 12 h. Food and water were available ad libitum. Whole-body SPECT/CT images were acquired at various times (20 min, 1 h 20, 3 h 20, 7 h 20, 26 h, 48 h) after tail vein injection of 8 MBq of radio-labelled $NaFe^{III}[Fe^{II}(CN)_6]$/grafted dextran, $^{201}Tl^{+}$/ $NaFe^{III}[Fe^{II}(CN)_6]$/lipid bilayers and $Au@NaNi[Fe^{II}(CN)_6]@$ $^{201}Tl^{+}$/ $NaFe^{III}[Fe^{II}(CN)_6]$/grafted dextran nanoprobes. Mice were anesthetized with 2% isoflurane and positioned on the bed of 4-head multiplexing multipinhole NanoSPECT camera (Bioscan Inc., Washington, USA). Energy window was centered at 73 keV with ± 20% width, acquisition times were defined to obtain 30,000 counts for each projection with 24 projections. Images and maximum intensity projections (MIPs) were reconstructed using the dedicated software Invivoscope® (Bioscan, Inc., Washington, USA) and Mediso InterViewXP® (Mediso, Budapest Hungary). Concurrent microCT whole-body images were performed for anatomic co-registration with SPECT data. Reconstructed data from SPECT and CT were visualized and co-registered using Invivoscope®. *In vivo* experiments were repeated three times, and quantification on whole body images provided semi-quantitative data.

Characterisation methods

Infrared spectra were recorded as KBr disks on a Nicolet Model 510P spectrophotometer. UV-Vis spectra were collected on a SPECOORD 210 UV-VIS spectrometer in water. Transmission Electron Microscopy (TEM) observations were carried out at 100 kV (JEOL 1200 EXII). Samples for TEM measurements were deposited from solutions on copper grids. Nanoparticles' size distribution histograms were determined using enlarged TEM micrographs taken at magnification of 100 K on a statistical sample of ca. 300 nanoparticles. HRTEM measurements were performed on a JEOL 2200FS.

CryoTEM experiments were performed using a JEOL 220FS transmission electron microscope (Japan) with a 4k x 4k slow-scan CCD camera (Gatan, USA), and the observations were carried out at 100 kV. Samples were prepared on Lacey carbon films on copper grids R 2/2 (Eloîse, France). Three microliters of NPs suspensions prepared at 3 mg/ml in HBS were applied to glow discharged Lacey grid (Ted Pella inc.), blotted for 1s and then flash frozen in liquid ethane using a CP3 cryo-plunge (Gatan inc.). Before freezing, the humidity rate was stabilized at about 95 %. Cryo-EM was carried out on a JEOL 2200FS FEG operating at 200 kV under low-dose conditions (total dose of 20 electrons/Å2) in the zero-energy-

loss mode with a slit width of 20 eV. Images were taken at a nominal magnification of 50,000 x corresponding to a calibrated magnification of 45,591 x with defocus ranging from 1.4 to 2.5 µm. Scanning Electronic Microscopy (EDS) analyses were performed on a FEI Quanta FEG 200 instrument. The powders were deposited on an adhesive carbon film and analysed under vacuum. The quantification of the heavy elements was carried out with the INCA software, with a dwell time of 3 µs. Hydrodynamic diameter and zeta potential were determined using a Nano ZS apparatus (Malvern). Data were collected from the He-Ne laser light source (633nm) at 173° from the transmitted beam. Results were presented as Z-average obtained in intensity mode, associated to the polydispersity index (PDI).

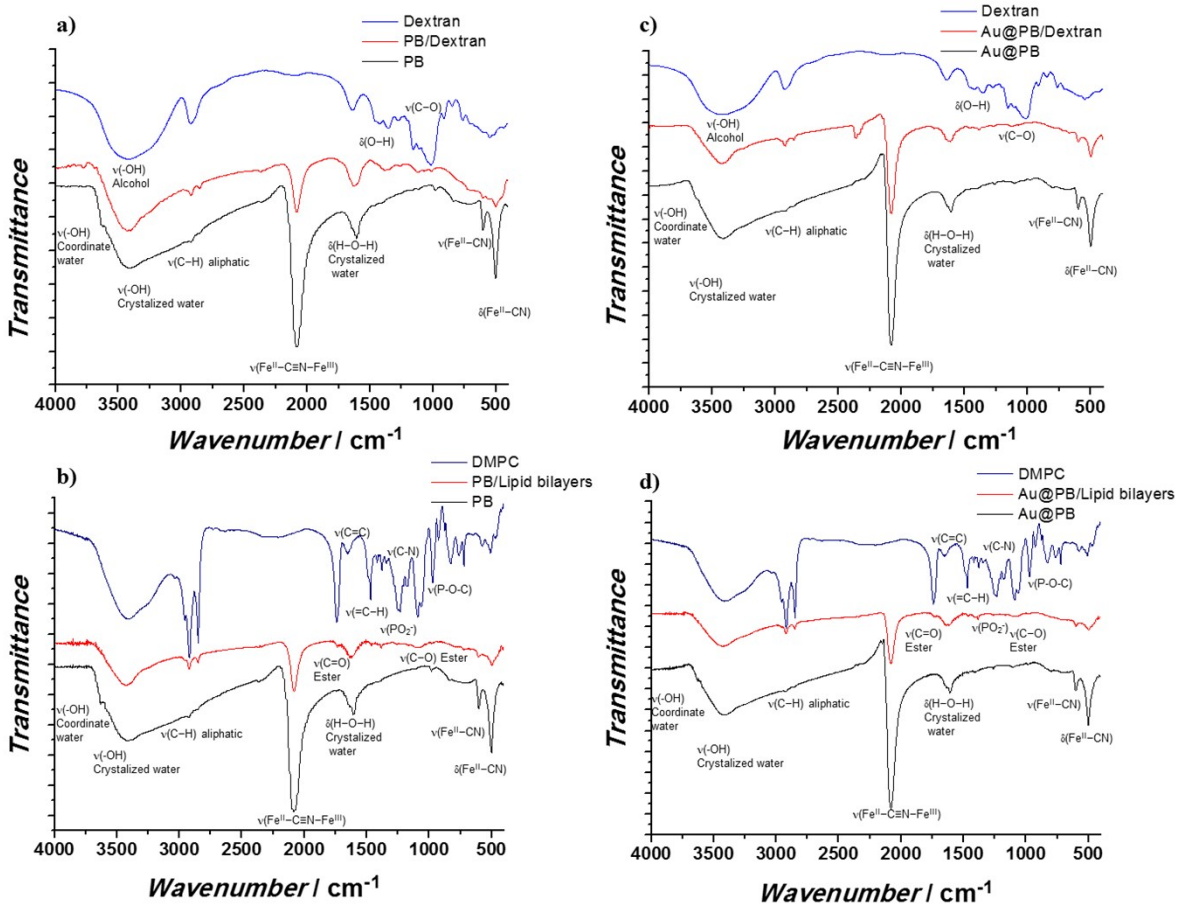

Fig. S1. a) IR spectra of PB nanoparticles **1**, PB nanoparticles coated with dextran **1a** and dextran; b) IR spectra of PB nanoparticles **1**, PB nanoparticles coated with lipid bilayers **1b** and DMPC; c) IR spectra of Au@PB nanoparticles **2**, nanoparticles grafted with dextran **2a** and dextran; d) IR spectra of Au@PB nanoparticles **2**, nanoparticles grafted with lipid bilayer **2b** and DMPC.

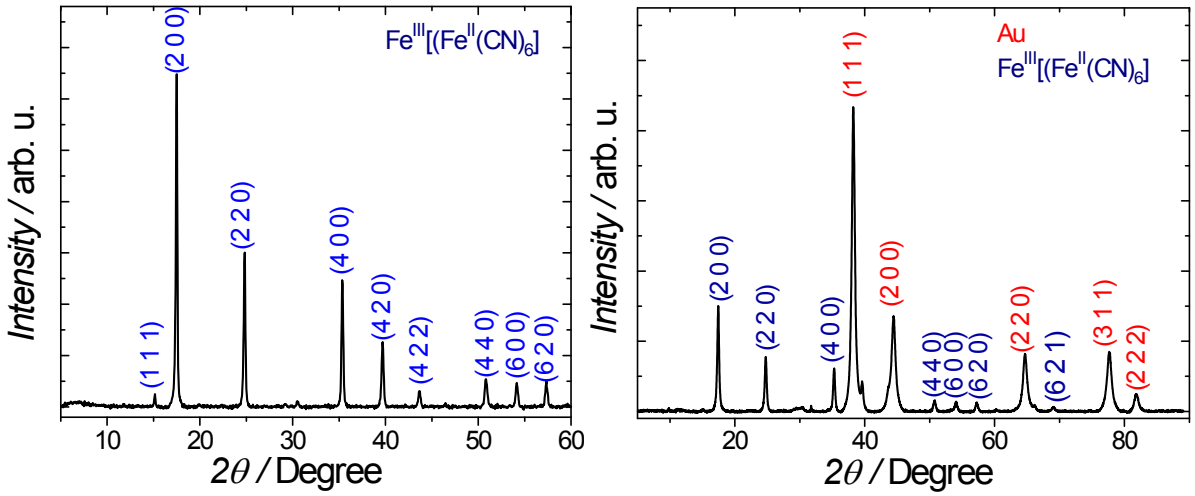

Fig. S2. PXRD pattern of the PB nanoparticles **1** (left) and of the core@shell nanoheterostuctures Au@PB **2** (right).

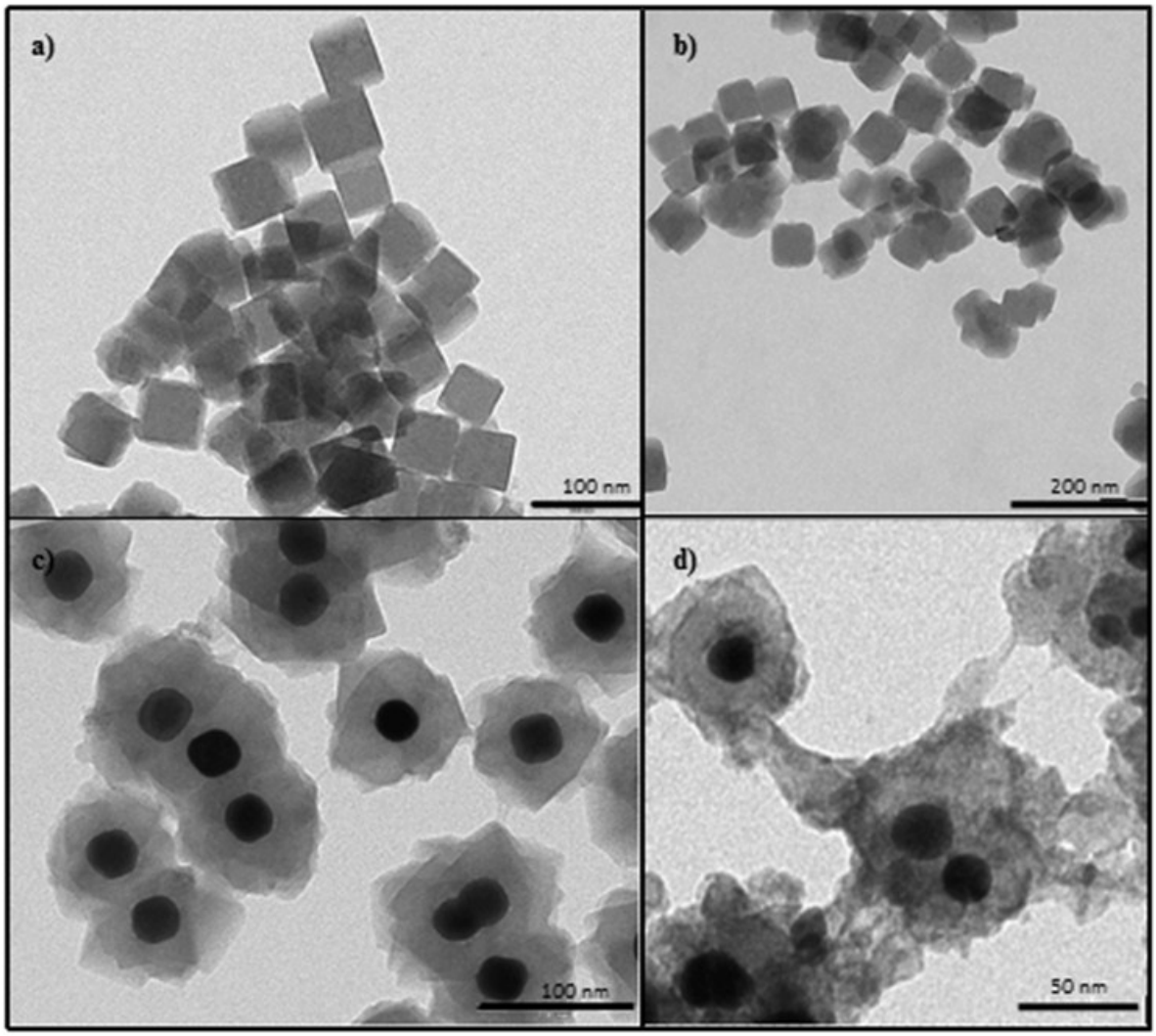

Fig. S3. TEM images of the native nanoparticles for: a) PB **1**; b) the PB/dextran **1a**; c) the core@shell nanoheterostuctures Au@PB **2**; d) the Au@PB/ dextran **2a**.

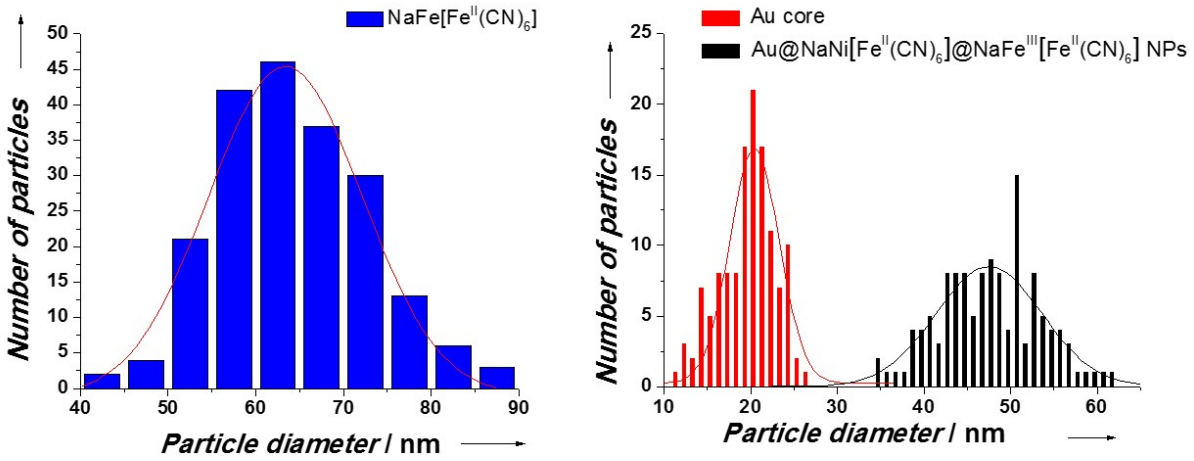

Fig.S4. Size distributions for: PB **1** (left), core@shell nanoheterostuctures Au@PB **2** (right).

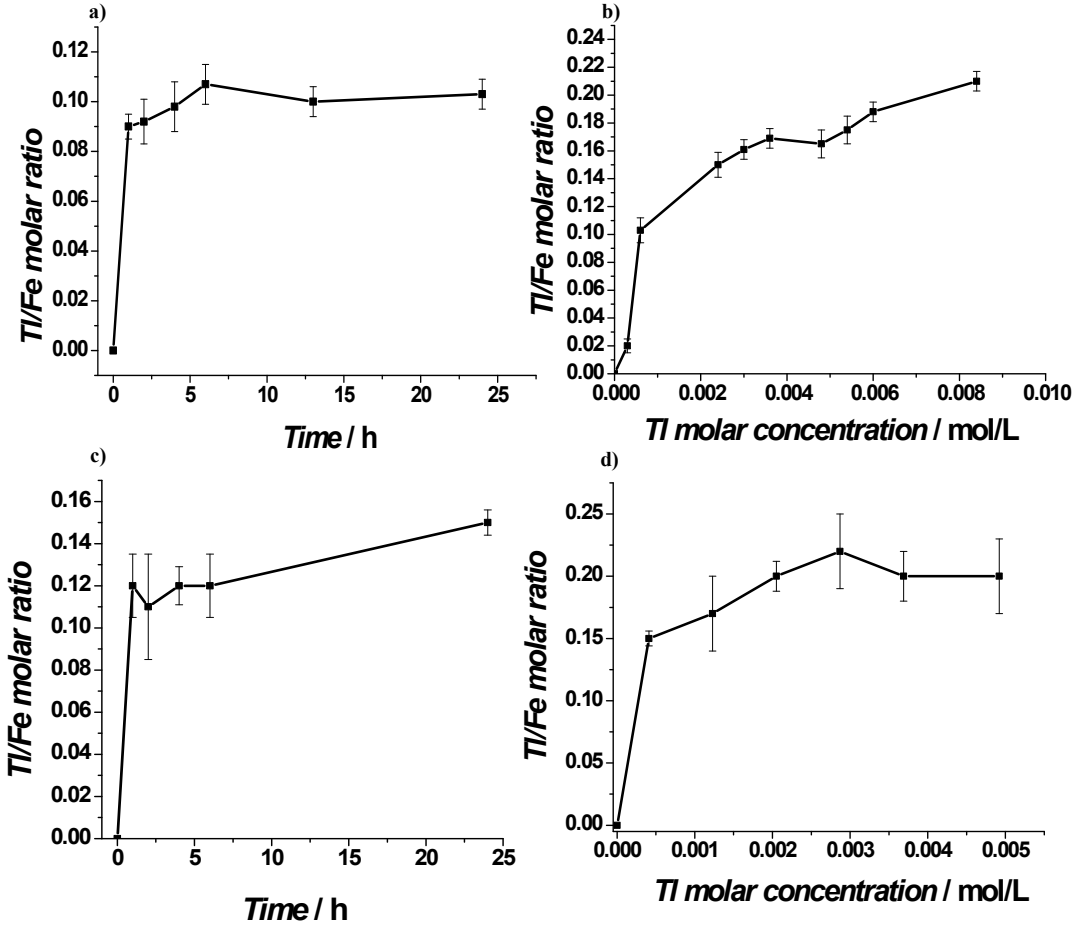

Fig. S5. a) isotherm and b) kinetic of Tl^+ absorption for the PB/dextran **1a**; c) kinetic and d) isotherm of Tl^+ absorption for the Au@PB/dextran **2a**.

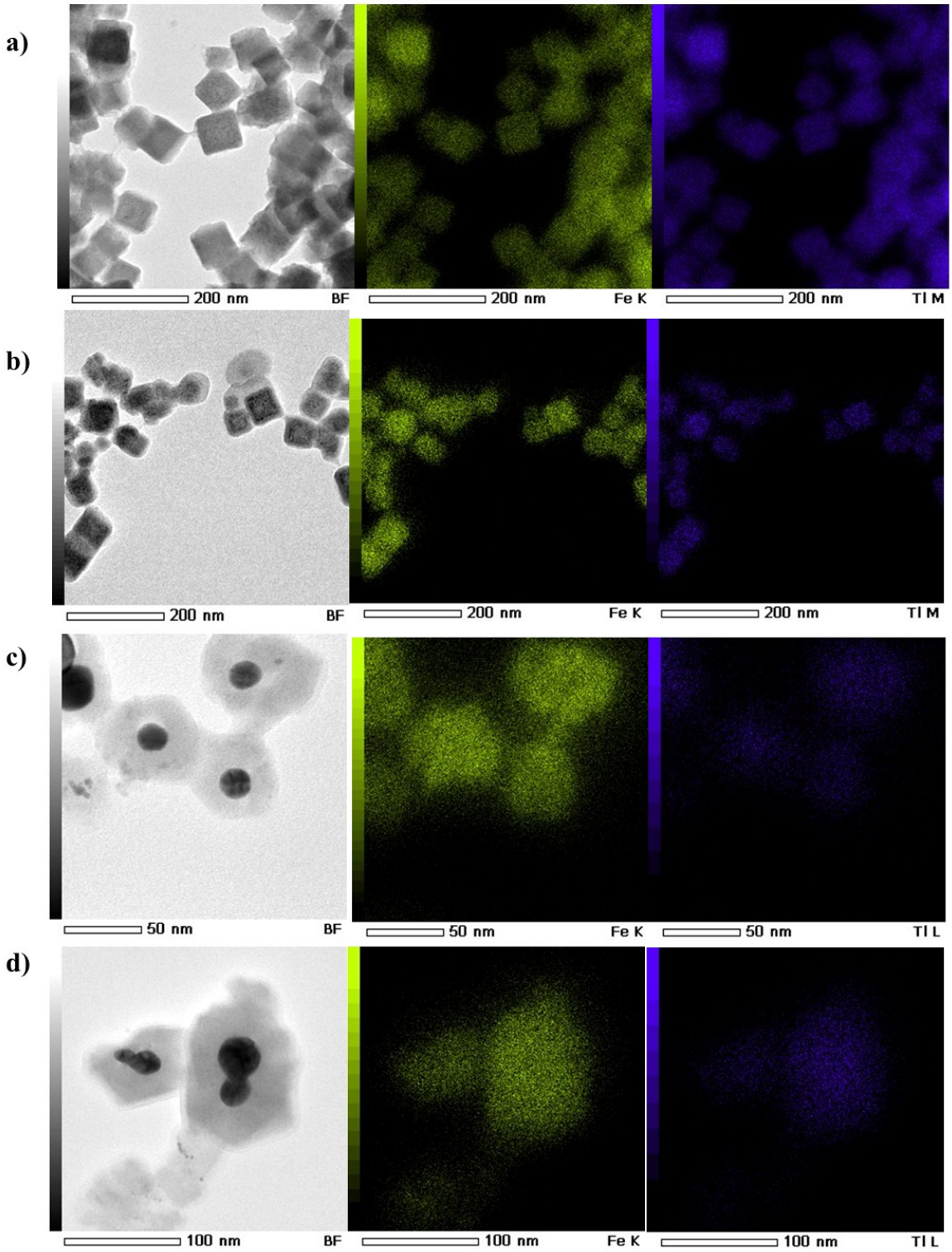

Fig. S6. STEM images and topochemical repartition (HAADF mode) of Fe (green) and Tl (blue) atoms for: a) PB/dextran nanoparticles **1a**; b) PB/lipid bilayers **1b**; c) Au@PB/dextran **2a** and d) Au@PB/lipid bilayers **2b**.

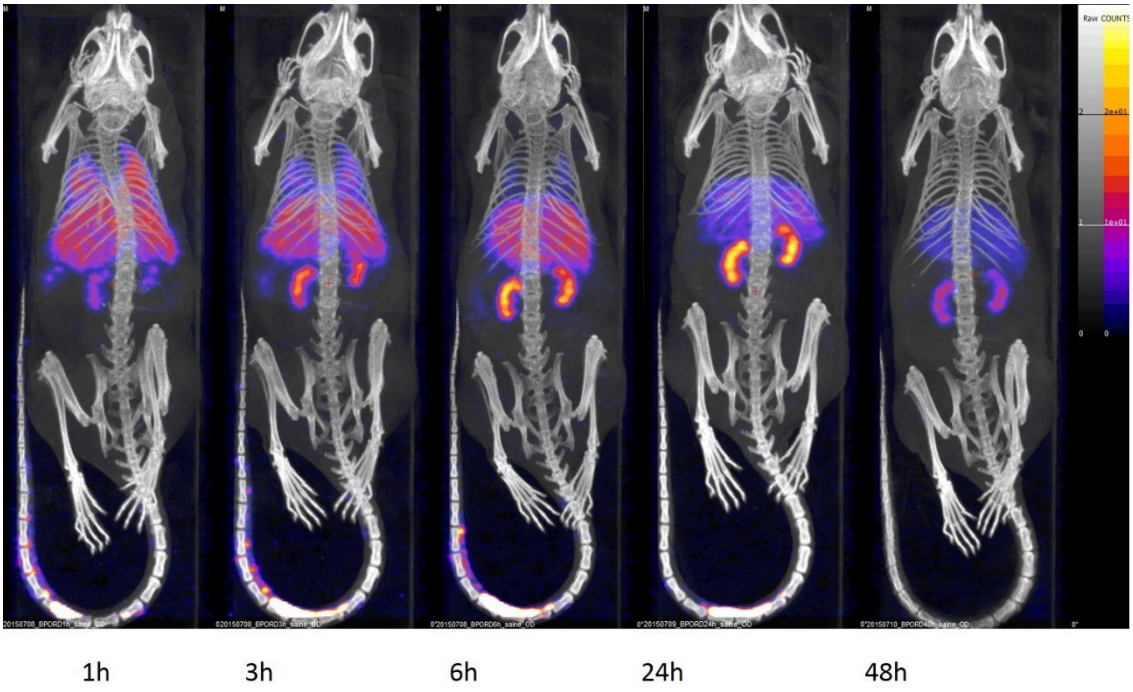

Fig. S7. SPECT/CT images shown as Maximum Intensity Projection (MIP) of the mice for different periods of time from 1h to 48h performed after *iv* injection of $^{201}Tl^{+}$**/2a** nanoprobes.

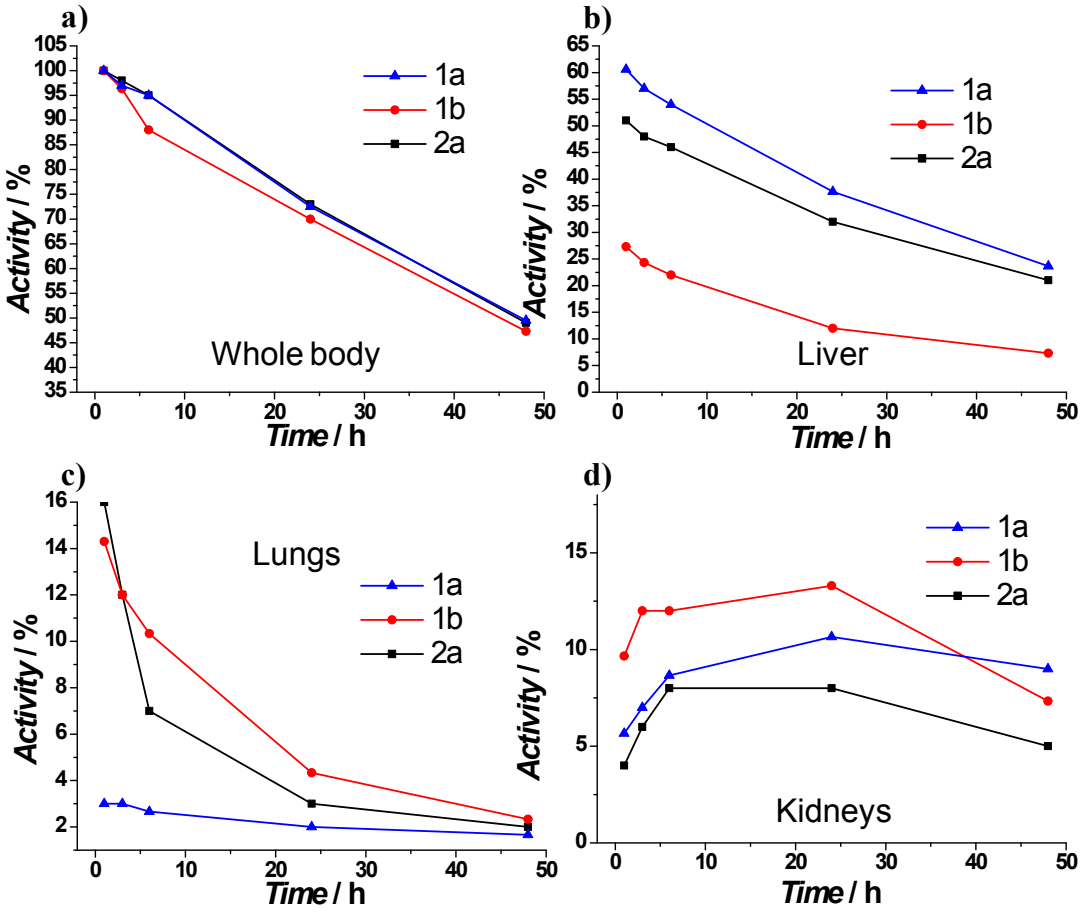

Fig. S8. Uptake curves by organ of interest in time after *iv* injection for NPs **1a**, **1b** and **2a**.

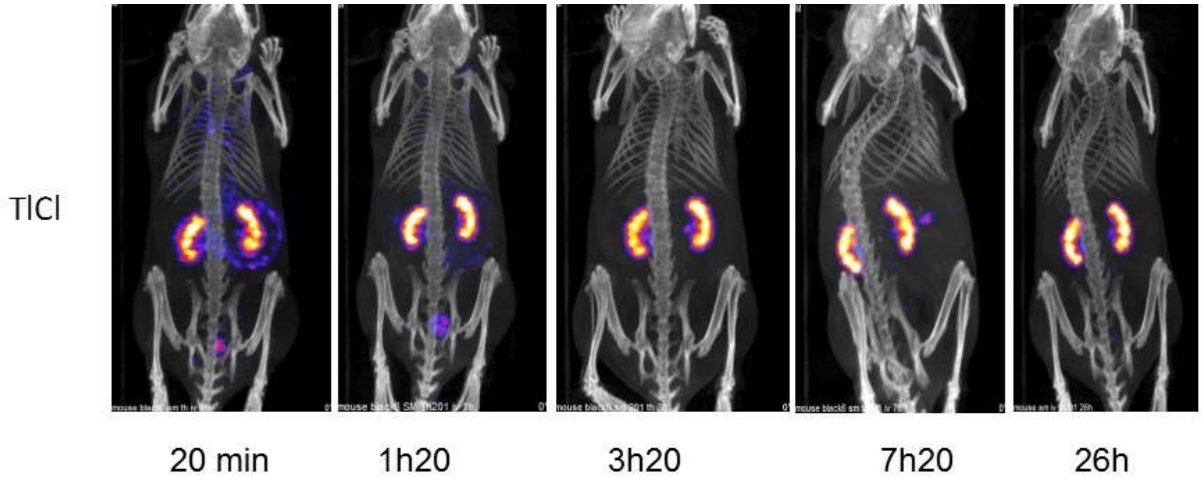

Fig. S9. SPECT/CT images shown as Maximum Intensity Projection (MIP) of the mice for different periods of time performed after *iv* injection of free ^{201}TlCl.